Expressing Eqs. (7) and (8) in the polar coordinates defined in Fig. 1 gives

$$v\cos\psi = v'\cos\psi' - v_s \tag{9}$$

$$v\sin\psi\,\cos\phi = v'\sin\psi'\,\cos\phi' \tag{10}$$

The azimuthal angles are unchanged by the coordinate transformation, so $\phi = \phi'$. Therefore Eq. (10) reduces to,

$$v\sin\psi = v'\sin\psi' \tag{11}$$

To solve for $V(\psi', v')$ square both Eqs. (9) and (11), add the results and take the square root to obtain

$$v = \left(v'^2 + v_s^2 - 2v'v_s\cos\psi'\right)^{\frac{1}{2}} \tag{12}$$

To solve for $V'(\psi', v)$, note that Eq. (12) squared is a quadratic equation for v' with the solution

$$v' = v_s\cos\psi' + \sqrt{v_s^2\cos^2\psi' - (v_s^2 - v^2)} \tag{13}$$

To solve for $\Psi(\psi', v')$, divide Eq. (9) by v and take the arccosine to get

$$\psi = \cos^{-1}\left(\frac{v'\cos\psi - v_s}{v}\right) \tag{14}$$

where the v in the denominator is given by Eq. (12).

Finally, the Jacobian is solved for by substituting Eqs. (14) and (12) into Eq. (6) to obtain

$$J = \frac{v'}{v} \tag{15}$$

With the above results, Eq. (5) can be further simplified. Replace the Jacobian with Eq. (15) and $h(\psi)$ with $(\sin\psi)/2$ and substitute Eq. (11) into the result to obtain

$$\int_0^{\pi}\int_{V'[\psi', v_{\min}]}^{V'[\psi', v_{\max}]} F_{\mathrm{sp}}\left(\frac{v'}{V[\psi', v']}\right)^3 A\,\Delta t \times g(V[\psi', v'])\frac{\sin\psi'}{2}\,\mathrm{d}v'\,\mathrm{d}\psi' \tag{16}$$

Equation (16) normalized by $F_{\mathrm{sp}}A\,\Delta t$ is the velocity focusing factor in orbiting spacecraft coordinates. That factor was numerically integrated and compared with Kessler's equation for the velocity focusing factor in stationary spacecraft coordinates, which is repeated as Eq. (2) in this paper. Agreement was obtained to within the tolerance set for the numerical integrations (six significant figures for the smallest tolerance calculated), confirming the accuracy of the coordinate transformations and the Jacobian derived here.

The mean number of impacts onto an oriented flat plate is obtained from Eq. (16) by multiplying the integrand of Eq. (16) by the area the flat plate presents to meteoroids. The presented area of the flat plate is equal to the product of the area A with the cosine of the angle β the meteoroid makes with respect to the plate normal. Therefore, the mean number of impacts onto an oriented flat plate is

$$\int_0^{\pi}\int_{V'[\psi', v_{\min}]}^{V'[\psi', v_{\max}]} F_{\mathrm{sp}}\left(\frac{v'}{V[\psi', v']}\right)^3 A[\cos\beta]^+\,\Delta t \times g(V[\psi', v'])\frac{\sin\psi'}{2}\,\mathrm{d}v'\,\mathrm{d}\psi' \tag{17}$$

The notation $[\ ]^+$ denotes that only impacts on the upside of the plate are counted, i.e., whenever $\cos\beta \leq 0$, set the quantity in square brackets equal to zero.

Equation (17) can be used to calculate the ratio of the flux on a forward-facing flat plate to the flux on an aft-facing flat plate, by taking the ratio of Eq. (17) evaluated from 0 to $\pi/2$ (instead of from 0 to π) to Eq. (17) evaluated from $\pi/2$ to π. Zook[3] obtained a ratio 7.2 for a flat plate at 460-km altitude and $g(v)$ given by Eq. (1), whereas a ratio 9.04 was obtained with Eq. (17), when Earth shadowing was taken into account.

Acknowledgment

This work was performed under NASA contract NAS8-50000.

References

[1]Frost, V. C., "Meteoroid Damage Assessment," NASA SP-8042, May 1970.

[2]Kessler, D. J., "A Guide to Using Meteoroid-Environment Models for Experiment and Spacecraft Design Applications," NASA TN D-6596, March 1972.

[3]Zook, H. A., "Deriving the Velocity Distribution of Meteoroids from the Measured Meteoroid Impact Directionality on the Various LDEF Surfaces," *LDEF—69 Months in Space, First Post-Retrieval Symposium*, NASA CP-3134, Part 1, 1991, pp. 569–580.

[4]Sullivan, K., and McDonnell, J. A. M., "LDEF Flux Anisotropy: Dynamic Modelling and Flux Transformations to Define the Interplanetary Micrometeoroid Environment," *Hypervelocity Impacts in Space*, University of Kent Press, Canterbury, England UK, 1993, pp. 126–132.

[5]Hawkins, G. S., and Southworth, R. B., "Statistics of Meteors in the Earth's Atmosphere," *Smithsonian Contributions to Astrophysics*, Vol. 2, No. 11, 1958, pp. 349–364.

[6]Erickson, J. E., "Velocity Distribution of Sporadic Photographic Meteors," *Journal of Geophysical Research*, Vol. 73, No. 12, 1968, pp. 3721–3726.

[7]Zook, H. A., "The State of Meteoritic Material on the Moon," *Proceedings of the Lunar Science Conference, 6th*, 1975, pp. 1653–1672.

Analytical Solution for Controls, Heats, and States of Flight Trajectories

Ahmed Z. Al-Garni*

King Fahd University of Petroleum and Minerals, Dhahran 31261, Saudi Arabia

Nomenclature

C_D = drag coefficient, where $C_{D_t} = C_{D_a} + C_{D_r}$
C_L = lift coefficient, where $C_{L_t} = C_{L_a} + C_{D_r}$
C_Q = heat constant = $1.83 \times 10^{-8} R_n^{-1/2}(1 - h'_W/h'_0)$, $(\mathrm{J/cm^2})/(\mathrm{kg/m^3})^{\frac{1}{2}}(m^3/s^3)$, for stagnation point, where R_n is in meters, h'_W = enthalpy at wall, and h'_0 = total enthalpy
D = drag, where $D_t = D_a + D_r$, N
E = aerodynamic-lift-to-aerodynamic-drag ratio, $L_3/D_a = C_{L_a}/C_{D_a}$
E^* = maximum E, $(L_a/D_a)_{\max} = C^*_{L_a}/C^*_{D_a}$
f_a = function of the aerodynamic control, $C_{D_a}/C^*_{L_a} = 1 + \lambda_a^2/2E^*$
f_t = function of the total aerodynamic control, where $f_t = f_a + f_r = 1 + \lambda_t^2/2E^*$
g = acceleration due to gravity, m/s²
h = geometric altitude from the earth's equator, km
I_{sp} = specific impulse, s
L = lift, where $L_t = L_a + L_r$, N
M = Mach number
m = mass of the vehicle at any time, kg
Q = heat load per unit area, kJ/cm²
r = position of the vehicle's mass center with respect to the earth's center, m or km
S = vehicle aerodynamic reference area, m²
T_t = total (or gross) thrust, N
T_n = net thrust, $T_t - D_r$, N
t = time, s

Received May 27, 1993; revision received May 16, 1994; accepted for publication May 17, 1994.

*Assistant Professor of Aerospace Engineering and Aeronautical Group Coordinator, Mechanical Engineering Department. Member AIAA.

V = magnitude of velocity of the vehicle's center of mass with respect to a noninertial reference frame fixed in and rotating with the earth, m/s
W = weight for the vehicle, N
α = angle of attack between T_t and V vectors
β = reciprocal of the scale height $\approx 0,000147\ \mathrm{m}^{-1}$
γ = flight-path angle of the vehicle, rad
ρ = atmospheric air density, kg/m^3
θ = longitudinal position of the vehicle measured from the reference axis X, in the equatorial plane, positive eastward, rad

Subscripts
a = aerodynamic, without the effect of ram drag
an = analytical
c = constant
f = final
i = initial
nu = numerical
r = due to ram drag
rc = constant reference value
t = total, including the effect of ram drag
0 = at earth surface

Superscript
$*$ = value at E^*

Introduction

THIS paper presents an extension to the work in Ref. 1, which deals with re-entry problems with only one control, i.e., aerodynamic lift modulation. Here, additional equations (relation between thrust and mass expulsion rate) and two controls (thrust and lift) are introduced.

This study addresses three cases of constant-constraint pairs: constant acceleration with constant rate of climb (case 1), constant acceleration with constant flight-path angle (case 2), and constant acceleration with constant dynamic pressure (case 3). For these cases, analytical closed-form solutions are derived for two nonlinear feedback controls, which are necessary to transfer a vehicle from one specified state to another. The solutions obtained are unique for a given set of constraints. Also derived are equations for the heat rate with the heat load for hypersonic speed (some similar heat results are reported in Refs. 2 and 3) and the integration of most state variables. The resulting equations apply to any flight vehicle [e.g., airplane, rocket, and aerospace plane (including vehicles with high aerodynamic-lift-to-aerodynamic-drag ratio such as wave riders)]. The results of this study will provide insights into the design and operation of flight vehicles. It also defines additional work needed in the area of trajectory and control.

Model Equation

The vehicle is modeled as a variable point mass with parabolic drag polar (plus a small addition to the lift due to the effect of the ram air at hypersonic speed) and variable lift and thrust, as described in Refs. 4–6, but with consideration for high angle of attack. The earth is assumed to be spherical and nonrotating with an exponential atmosphere. The trajectory is taken in the equatorial plane. With the above assumptions the equations that describe the system are given by

$$\frac{\mathrm{d}r}{\mathrm{d}t} = V\sin\gamma = rc \tag{1}$$

$$\frac{\mathrm{d}\rho}{\mathrm{d}t} = -\rho\beta V\sin\gamma \tag{2}$$

$$\frac{\mathrm{d}V}{\mathrm{d}t} = \frac{T_t\cos\alpha - D_t}{m} - g\sin\gamma \tag{3}$$

$$V\frac{\mathrm{d}\gamma}{\mathrm{d}t} = \frac{L_t}{m} + \frac{T_t\sin\alpha}{m} - g\cos\gamma + \frac{V^2}{r}\cos\gamma \tag{4}$$

$$\frac{\mathrm{d}\theta}{\mathrm{d}t} = \frac{V}{r}\cos\gamma \tag{5}$$

$$\frac{\mathrm{d}m}{\mathrm{d}t} = -\frac{T_t}{I_{sp}g_0} \tag{6}$$

$$\frac{\mathrm{d}Q}{\mathrm{d}t} = C_Q\rho^{0.5}V^3 \tag{7}$$

for hypersonic speed, and

$$q = \tfrac{1}{2}\rho V^2 \tag{8}$$

We should note that Eqs. (5) and (7) are not coupled with Eqs. (1–4) and (6); also Eqs. (1) and (2) can replace each other.

Introducing the dimensionless variables:

$$\hat{r} = \frac{r}{r_0} \tag{9a}$$

$$\eta = C_1 C_{L_a}^*\left(\frac{\rho}{\rho_0}\right) \tag{9b}$$

$$u = \frac{V^2}{\sqrt{g_0 r_0}} = \frac{V}{V_c} \tag{9c}$$

$$\mu = \frac{m}{m_0} \tag{9d}$$

$$\hat{t} = \frac{t}{t_c} \tag{9e}$$

where $t_c = \sqrt{r_0/g_0}$ and C_1 is a dimensionless arbitrary constant, used for pure computational numerical stability. The following dimensionless variables are also defined: $a = \mathrm{d}V/\mathrm{d}t/g_0$, which is the component of the dimensionless acceleration in the direction of the vehicle velocity; $\hat{\gamma} = \gamma/\gamma_{re}$, $\hat{\theta} = \theta/\theta_{re}$, $\widehat{rc} = rc/V_c$, where the constant values for γ_{re} and θ_{re} can be chosen arbitrarily; $\hat{q} = q/q_{re}$, where $q_{re} = C_3 = \rho_0 V_c^2/2C_1C_{L_a}^*$ in atmospheres or N/m^2; and $\hat{Q} = Q/Q_{re}$, where Q_{re} is a reference constant, which can be taken to be equal to the shuttle re-entry maximum value $\approx 50\ \mathrm{kJ/cm^2}$.

The dimensionless controls are

$$\lambda_a = \frac{C_{L_a}}{C_{L_a}^*} \tag{9f}$$

$$\lambda_r = d_1\lambda_a \tag{9g}$$

$$\lambda_t = \lambda_a + \lambda_r \tag{9h}$$

$$\tau_t = \frac{T_t}{W_0} \tag{9i}$$

$$\tau_n = \frac{T_t - D_r}{W_0} \tag{9j}$$

where d_1 is a dimensionless optimized coefficient for lift due to the component of total thrust control in the direction of lift, λ_t is the total dimensionless aerodynamic control, and τ_n is the net dimensionless thrust control. At hypersonic speeds D_r can be chosen as a function of T_t.

Applying the dimensionless variables $\hat{\gamma}, \hat{\theta}, \widehat{rc}, \hat{q}$, in (9a–9j) to Eqs. (1–8) yields

$$\frac{\mathrm{d}\hat{r}}{\mathrm{d}\hat{t}} = \dot{r}\left(\frac{t_c}{r_0}\right) = u\sin\gamma \tag{10}$$

$$\frac{\mathrm{d}\eta}{\mathrm{d}\hat{t}} = (\dot{\eta}t_c) = -\beta r_0\eta u\sin\gamma \tag{11}$$

$$\frac{\mathrm{d}u}{\mathrm{d}\hat{t}} = \dot{u}t_c = \left[\frac{\tau_t\cos\alpha}{\mu} - \left(\frac{C_4 r_0}{2C_1C_2}\right)f_t\left(\frac{\eta u^2}{\mu}\right) - \frac{\sin\gamma}{\hat{r}^2}\right] \tag{12}$$

where C_2 is the total characteristic constant length of the vehicle (in meters) and $C_4 = \rho_0 S C_2/m_0$ is a dimensionless constant, and

$$\frac{\mathrm{d}\hat{\gamma}}{\mathrm{d}\hat{t}} = \dot{\gamma}\left(\frac{t_c}{\gamma_{\mathrm{re}}}\right) = \frac{1}{\gamma_{\mathrm{re}}}\left[\frac{C_4 r_0}{2C_1C_2}\lambda_t\left(\frac{\eta u}{\mu}\right) + \left(\frac{\tau_t \sin\alpha}{\mu u}\right) - \frac{\cos\gamma}{\hat{r}^2 u} + \frac{u}{\hat{r}}\cos\gamma\right] \tag{13}$$

$$\frac{\mathrm{d}\hat{\theta}}{\mathrm{d}\hat{t}} = \dot{\theta}\left(\frac{t_c}{\theta_{\mathrm{re}}}\right) = \frac{1}{\theta_{\mathrm{re}}}\left(\frac{u}{\hat{r}}\cos\gamma\right) \tag{14}$$

$$\frac{\mathrm{d}\mu}{\mathrm{d}\hat{t}} = \dot{\mu}t_c = -t_c\frac{\tau_t}{I_{\mathrm{sp}}} \tag{15}$$

$$\frac{\mathrm{d}\hat{Q}}{\mathrm{d}\hat{t}} = \dot{Q}\left(\frac{t_c}{Q_{\mathrm{re}}}\right) = \frac{C_Q C_5 V_c^2 r_0 \eta^{0.5} u^3}{Q_{\mathrm{re}}} \tag{16}$$

$$\hat{q} = \eta u^2 \tag{17}$$

where $C_5 = \sqrt{\rho_0/C_2 C_{L_a}^*}$ is a constant with units of $(\mathrm{kg/m^3})^{1/2}$

Analytical Approach

For given $\mathrm{d}X_j/\mathrm{d}t = \dot{X}_j = f_j(\boldsymbol{X}, \boldsymbol{C}, t)$, $j = 1, 2, \ldots, n$ where $\boldsymbol{X}$ is the state vector of the nonlinear system and $\boldsymbol{C} \in C^{m'}$ is the control vector. To find the control vector such that the constraints $\Phi_\ell(\boldsymbol{X}, \boldsymbol{C}) =$ constant, $\ell = 1, 2, \ldots, p'$, $p' < n$ and $p' \leq m'$, are satisfied, if the system is controllable, then

$$\sum_{j=1}^{n} \frac{\partial \Phi_\ell}{\partial X_j} f_j(\boldsymbol{X}, \boldsymbol{C}) = 0 \tag{18}$$

where n is the number of equations, and m' is the number of controls. This, in general, generates, a trajectory that is not unique. The selection of the controls will be based on the mission desirability and physical constraints (e.g., $u_{f,\min} < u_f < u_{f,\max}$).

Consider as an example case 1, with Eqs. (1–8) or (10–17) and two constant constraints—constant acceleration Φ_1 with constant rate of climb Φ_2, (a_c, rc_c):

$$\Phi_1 = \frac{\mathrm{d}u}{\mathrm{d}t} = \frac{g_0 a_c}{V_c} \tag{19}$$

$$\Phi_2 = rc = V_c u \sin\gamma = rc_c \tag{20}$$

To obtain the controls, apply Eq. (18) to Eq. (20) and substitute for $\dot{u}$ from Eq. (19) and $\dot{\gamma}$ from Eq. (13); then, solving for λ_t, the following closed-form expression for the nonlinear feedback controls is obtained:

$$\lambda_t = \frac{m_0}{S}\left(\frac{2C_1\mu}{\rho_0 V_c \eta u^2}\right) \times \left(-\frac{g_0 a_c \tan\gamma}{V_c} - \frac{g_0 \tau_t \sin\alpha}{V_c \mu} + \frac{g_0\cos\gamma}{V_c \hat{r}^2} - \frac{V_c u^2 \cos\gamma}{r_0 \hat{r}}\right) \tag{21}$$

Equations (12) and (19) yield

$$\tau_t = \frac{1}{\cos\alpha}\left[\mu a_c + \left(\frac{S}{m_0}\right)\frac{\rho_0 V_c^2 f_t(\lambda_t)\eta u^2}{2C_1 g_0} + \frac{\mu \sin\gamma}{\hat{r}^2}\right] \tag{22}$$

After replacing r_0 by $V_c t_c$ in Eq. (16) and changing the independent variable from $\hat{t}$ to u with the use of Eqs. (19) and (16), the heat rate becomes

$$\frac{\mathrm{d}\hat{Q}}{\mathrm{d}u} = \left(\frac{\mathrm{d}\hat{Q}}{\mathrm{d}\hat{t}}\right)\left(\frac{\mathrm{d}\hat{t}}{\mathrm{d}u}\right) = \frac{C_Q C_5 V_c^4 \eta^{0.5} u^3}{Q_{\mathrm{re}} g_0 a_c} \tag{23}$$

This equation cannot be integrated unless we express η as a function of u. This can be done as follows: From Eqs. (11) and (20), we have

$$\frac{\mathrm{d}\eta}{\mathrm{d}\hat{t}} = -(\beta \eta rc_c)t_c \tag{24}$$

Changing the independent variable in Eq. (24) from $\hat{t}$ to u with the use of Eq. (19) gives

$$\frac{\mathrm{d}\eta}{\mathrm{d}u} = \left(\frac{\mathrm{d}\eta}{\mathrm{d}\hat{t}}\right)\left(\frac{\mathrm{d}\hat{t}}{\mathrm{d}u}\right) = -\frac{\beta V_c \eta rc_c}{g_0 a_c}$$

Rearranging this equation and integrating yields

$$\eta = \eta_i \exp\left(-\frac{\beta V_c rc_c}{g_0 a_c}(u - u_i)\right) = \eta(u) \tag{25}$$

This equation can be used to replace η as a function of u in Eq. (23), which after rearrangement gives

$$\frac{\mathrm{d}\hat{Q}}{\mathrm{d}u} = \frac{C_8 u^3 e^{C_7 u}}{Q_{\mathrm{re}}} \tag{26}$$

The integration of Eq. (26) yields the dimensionless heat load:

$$\hat{Q} = \frac{Q_i}{Q_{\mathrm{re}}} + \frac{1}{Q_{\mathrm{re}}}\left(\frac{C_8}{C_7^4}\right) \times \Big\{ -e^{-C_7 u_f}\big[(C_7 u_f)^3 + 3(C_7 u_f)^2 + 6(C_7 u_f) + 3!\big] + e^{-C_7 u_i}\big[(C_7 u_i)^3 + 3(C_7 u_i)^2 + 6(C_7 u_i) + 3!\big]\Big\} \tag{27}$$

where the constants are $C_6 = C_Q C_5 V_c^4/g_0 a_c$ (same units as C_Q), $C_7 = \beta V_c rc_c/2g_0 a_c$ (dimensionless), and $C_8 = C_6 \eta_i^{0.5} e^{C_7 u_i}$ (same units as C_Q).

Integration and Approximation of State Variables

From Eqs. (19) and (20), we have $\mathrm{d}\hat{r}/\mathrm{d}u = rc_c V_c/r_0 g_0 a_c = rc_c/V_c a_c = \widehat{rc}_c/a_c$, which by integration gives

$$r = r_i + \left(\frac{rc_c V_c}{g_0 a_c}\right)(u - u_i), \quad \text{or} \quad \hat{r} = \hat{r}_i + \left[\frac{\widehat{rc}_c}{a_c}(u - u_i)\right] \tag{28}$$

Integration of Eq. (19) gives

$$u = u_i + \left(\frac{a_0 a_c}{V_c}\right)t, \qquad \text{or} \quad u = u_i + a_c \hat{t} \tag{29}$$

From Eqs. (11) and (19), we have

$$\frac{\mathrm{d}\eta}{\mathrm{d}u} = -\frac{\beta \eta rc_c}{g_0 a_c/V_c}$$

which by integration gives

$$\eta = \eta_i \exp\left[-\frac{\beta V_c rc_c}{g_0 a_c}(u - u_i)\right], \qquad \text{or} \qquad \eta = \eta_i \exp\left[-\frac{\beta r_0 rc_c}{a_c}(u - u_i)\right] \tag{30}$$

From Eq. (20), we have $\sin\gamma = rc_c/V_c u$. This yields

$$\gamma = \sin^{-1}\left(\frac{rc_c}{V_c u}\right), \quad \text{or} \quad \hat{\gamma} = \frac{\sin^{-1}(\widehat{rc}_c/u)}{\gamma_{\mathrm{re}}} \tag{31}$$

First-order approximations of μ and θ for cases 1–3, give

$$\mu \approx \mu_i - a_m t, \qquad \text{or} \quad \mu \approx \mu_i - a_m t_c \hat{t} \tag{32}$$

$$\theta \approx \theta_i + a_m t, \qquad \text{or} \quad \hat{\theta} \approx \hat{\theta}_i + \frac{a_m t_c \hat{t}}{\theta_{\mathrm{re}}} \tag{33}$$

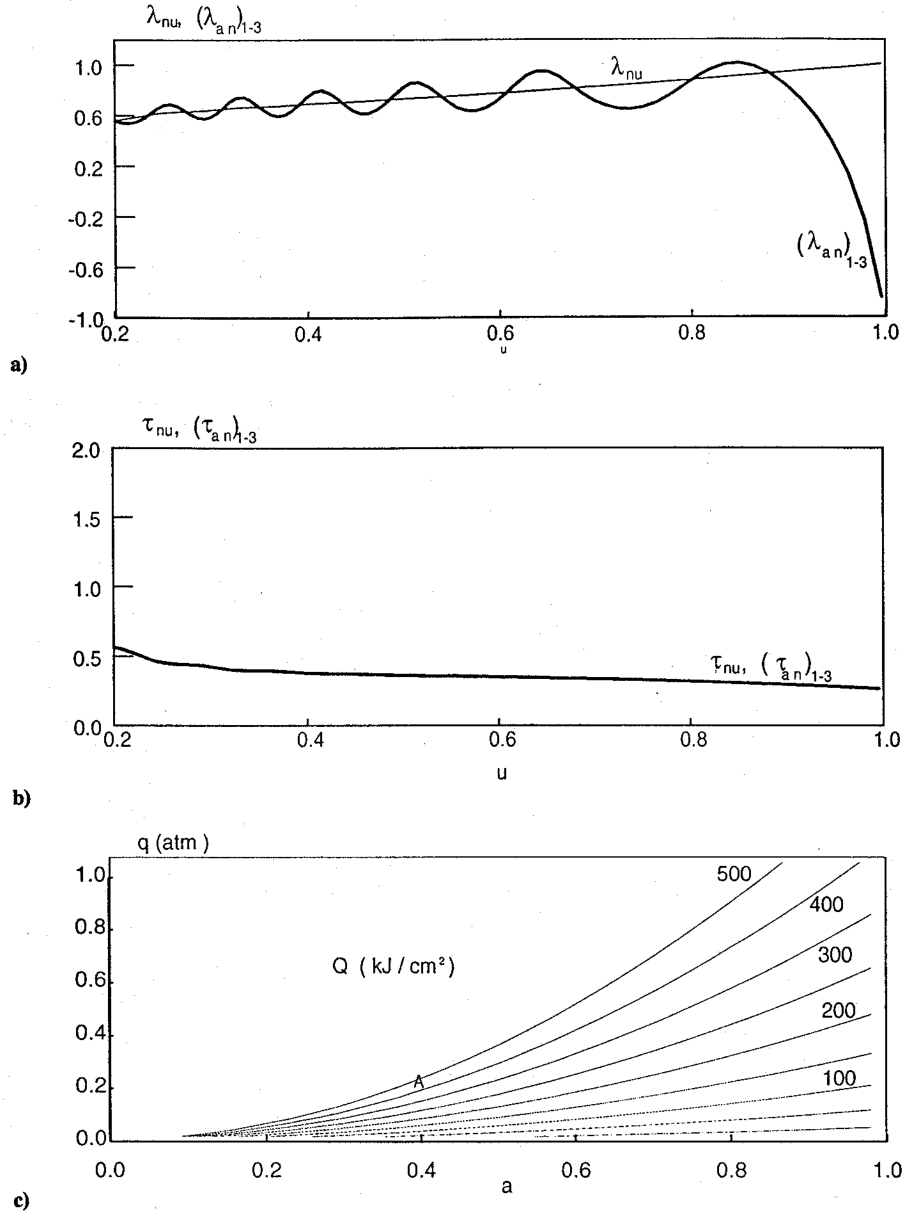

Fig. 1 Comparison between a) $(\lambda_t)_{an}$ of case 1-3 and $(\lambda_t)_{nu}$, adapted from Refs. 5 and 6 for small α; b) $(\hat{\tau})_{an}$ of cases 1-3 and $(\lambda_t)_{nu}$ adapted from Refs. 5 and 6 for small α; and c) contours for the analytical heat load Q_{an} in the range 0–500 kJ/cm^2, on the plane of the parameters a and q (case 3), adapted from Ref. 5; the point A at $a = 0.4$g and $q = 0.2$ atm represents the results of Ref. 2.

Also, we can specify the time or choose it for first-order approximation as a function of rc, and we can choose (for example, in the ascent of an aerospace plane to orbit) $a_m = 0.0005\ \mathrm{s}^{-1}$. This is justified in Ref. 5 by integrating the general equations of motion. Thus, for a specified time, Eqs. (21–33) give $\lambda_t = \lambda_t(a_c, r_c)$, $\tau_t = \tau_t(a_c, rc_c)$, and $\hat{Q}_t = \hat{Q}_t(a_c, rc_c)$.

We now consider case 2—constant acceleration Φ_1 with constant flight-path angle Φ_2, (a_c, γ_c):

$$\Phi_1 = \frac{du}{dt} = \frac{g_0}{V_c}a_c \tag{34}$$

$$\dot{\Phi}_2 = \frac{d\gamma_c}{dt} = 0 \tag{35}$$

$$\lambda_t = \frac{m_0}{S}\left(\frac{2C_1\mu\cos\gamma_c}{\rho_0\eta}\right)\left(\frac{\tau_t\sin\alpha}{r_0\cos\gamma_c\mu u^2} + \frac{g_0}{V_c^2u^2\hat{r}^2} - \frac{1}{r_0\hat{r}}\right) \tag{36}$$

$$\tau_t = \frac{1}{\cos\alpha}\left[\mu a_c + \left(\frac{S}{m_0}\right)\frac{\rho_0 V_c^2 f_t(\lambda_t)\eta u^2}{2C_1 g_0} + \frac{\mu\sin\gamma_c}{\hat{r}^2}\right] \tag{37}$$

$$\hat{Q}^2 \le \frac{Q_i}{Q_{re}} + \left(\frac{1}{Q_{re}}\right)\frac{C_{10}}{u_i}\left(\frac{3}{2^3C_9^2}\sqrt{\frac{\pi}{C_9}}\right) \tag{38}$$

where the constants are $C_9 = \beta V_c^2(\sin\gamma_c)/(4g_0a_c)$ (dimensionless) and $C_{10} = C_6\eta_i^{0.5}e^{C_9u_i^2}$ (same units as C_Q), and the heat-rate equation is given by Eq. (16) after replacing r_0 by V_ct_c:

$$\hat{r} = \hat{r}_i + \frac{\sin\gamma_c}{2a_c}(u^2 - u_i^2) \tag{39}$$

$$\eta = \eta_i\exp\left[-\left(\frac{3r_0\sin\gamma_c}{a_c}\right)\frac{u^2 - u_i^2}{2}\right] \tag{40}$$

$$u = u_i + a_c\hat{t} \tag{41}$$

$$\hat{\gamma} = \hat{\gamma}_c - \text{constant} \tag{42}$$

Finally we consider case 3—constant acceleration Φ_1 with constant dynamic pressure, $\Phi_1(a_c, q_c)$:

$$\Phi_1 = \frac{du}{dt} = \frac{g_0}{V_c}a_c, \qquad \Phi_2 = q = C_3\eta u^2 = q_c \tag{43}$$

$$\lambda_t = \frac{m_0}{S}\left(\frac{2C_1C_3\mu}{\rho_0 V_c q_c}\right)\left(-\frac{2g_0 a_c \tan\gamma}{V_c} - \frac{g_0\tau_t \sin\alpha}{V_c\mu} + \frac{g_0\cos\gamma}{V_c\hat{r}^2} - \frac{V_c q_c \cos\gamma}{C_3 r_0 \eta \hat{r}}\right) \tag{44}$$

for $q_c \neq 0$,

$$\tau_t = \frac{1}{\cos\alpha}\left[\mu a_c + \left(\frac{S}{m_0}\right)\frac{\rho_0 f_t(\lambda_t)V_c^2 q_c}{2C_1C_3g_0} + \frac{\mu\sin\gamma}{\hat{r}^2}\right] \tag{45}$$

$$\hat{Q} = \frac{Q_i}{Q_{re}} + \frac{C_Q C_5 V_c^4}{Q_{re} g_0 a_c}\sqrt{\frac{q_c}{C_3}}\left(\frac{u_f^3 - u_i^3}{3}\right) \tag{46}$$

for $a_c \neq 0$.

We have used Eq. (16) for the heat rate, replacing $r_0\eta^{0.5}$ by $V_c\sqrt{q_c/C_3t_c}$. Finally,

$$\hat{r} = \hat{r}_i + \frac{2}{\beta r_0}\ln\left(\frac{u}{u_i}\right) \tag{47}$$

$$\eta = \eta_i\left(\frac{u_i}{u}\right)^2 \tag{48}$$

$$u = u_i + \left(\frac{g_0 a_c}{V_c}\right)t_c\hat{t} \tag{49}$$

$$\hat{\gamma} = \frac{\sin^{-1}\left(2a_c/\beta r_0 u^2\right)}{\gamma_{re}} \tag{50}$$

Results

The results for the controls, heats, and state variables of cases 1–3 are given in Eqs. (16), (21–22), (27–33), (36–42), and (44–50). Some of the results from Refs. 5 and 6 for small angle of attack are plotted in Fig. 1 to show how well the present results agree with the numerical solutions. These results are for the aerospace plane ascending to orbit. In Fig. 1a we have the aerodynamic controls λ_{nu} and λ_{an} for the numerical solution and the analytical solution of cases 1–3, respectively. This shows λ_{nu} and λ_{an} are in close agreement (e.g., $0.55 \leq \lambda \leq 1.1$ for $0.2 \leq u \leq 0.9$). In Fig. 1b, we have the total thrust controls τ_{nu} and τ_{an} for the numerical solution and the analytical solution of cases 1–3, respectively. This figure shows τ_{nu} and τ_{an} are almost the same. Also, the comparison of the heat-load contours on the q-a plane in Fig. 1c at point A (i.e., $q = 0.2$ atm and $a = 0.4$g, where $Q \approx 400$(kJ/cm^2) is in agreement with the results of Ref. 2. Moreover, the results in Fig. 1c are more general than the results in Ref. 2, since the whole mapping of Q in the q-a plane is considered. Also, these results are close to the numerical results for the general system in Ref. 5, where $Q \approx 400$ kJ/cm^2.

Discussion and Conclusions

This paper has presented new closed-form analytical solutions for the nonlinear aerodynamic and thrust controls in feedback form for high angle of attack. Three cases were presented, each for a given pair of constraints (i.e., constant acceleration with constant rate of climb, constant acceleration with constant flight-path angle, and constant acceleration with constant dynamic pressure). Also presented where analytical solutions for heat rate and heat load (for hypersonic flight) and most of the state variables. comparisons with numerical results from Refs. 5 and 6 showed good agreement.

The results of the three cases presented herein can be used during various intervals of the trajectory to simulate and approximate the more general case.

References

[1]Blestos, N. A., "Performance and Control with Lift Modulation of Hypersonic Entry Vehicles," Ph.D. Dissertation, Dept. of Aerospace Engineering, Univ. of Michigan, Ann Arbor, MI, 1976.

[2]Tauber, M. E., and Menees, G. P., "Aerothermodynamics of Transatmospheric Vehicles," AIAA Paper 86-1257, June 1986.

[3]Anderson, John D., Jr., *Hypersonic and High Temperature Gas Dynamics*, McGraw-Hill, New York, 1989, pp. 291, 292.

[4]Vinh, N. X., *Optimal Trajectories in Atmospheric Flight*, Elsevier, New York, 1981, pp. 15–50.

[5]Al–Garni, A. Z., "Performance and Control of Ascending Trajectories to Minimize Heat Load for Transatmospheric Aerospace Planes," Ph.D. Dissertation, Dept. of Aerospace Engineering, Univ. of Maryland, College Park, MD, Aug. 1991.

[6]Barlow, J., and Al–Garni, A., "Ascending Trajectories Performance and Control to Minimize Heat Load for Transatmospheric Aerospace Planes," AIAA Atmospheric Flight Mechanics Conference, Paper AIAA-90-2828, Aug. 1990.